

Article

SPI Drought Class Predictions Driven by the North Atlantic Oscillation Index Using Log-Linear Modeling

Elsa E. Moreira ^{1,*}, Carlos L. Pires ² and Luís S. Pereira ³

¹ Center of Mathematics and Applications (CMA), Faculty of Sciences and Technology, New University of Lisbon, Caparica 2829-516, Portugal

² Instituto Dom Luiz (IDL), Faculty of Sciences, University of Lisbon, Lisboa 1749-016, Portugal; clpires@fc.ul.pt

³ Research Center for Landscape, Environment, Agriculture and Food (LEAF), Institute of Agronomy, University of Lisbon, Lisbon 1349-017, Portugal; lspereira@isa.ulisboa.pt

* Correspondence: efm@fct.unl.pt; Tel.: +351-212-948-300 (ext. 10867)

Academic Editor: Athanasios Loukas

Received: 13 October 2015; Accepted: 27 January 2016; Published: 30 January 2016

Abstract: This study aims at predicting the Standard Precipitation Index (SPI) drought class transitions in Portugal, considering the influence of the North Atlantic Oscillation (NAO) as one of the main large-scale atmospheric drivers of precipitation and drought fields across the Western European and Mediterranean areas. Log-linear modeling of the drought class transition probabilities on three temporal steps (dimensions) was used in an SPI time series of six- and 12-month time scales (SPI6 and SPI12) obtained from Global Precipitation Climatology Centre (GPCC) precipitation datasets with 1.0 degree of spatial resolution for 10 grid points over Portugal and a length of 112 years (1902–2014). The aim was to model two monthly transitions of SPI drought classes under the influence of the NAO index in its negative and positive phase in order to obtain improvements in the predictions relative to the modeling not including the NAO index. The ratios (*odds ratio*) between transitional probabilities and their confidence intervals were computed in order to estimate the probability of one drought class transition over another. The prediction results produced by the model with the forcing of NAO were compared with the results produced by the same model without that forcing, using skill scores computed for the entire time series length. Overall results have shown good prediction performance, ranging from 73% to 76% in the percentage of corrects (PC) and 56%–62% in the Heidke skill score (HSS) regarding the SPI6 application and ranging from 82% to 85% in the PC and 72%–76% in the HSS for the SPI12 application. The model with the NAO forcing led to improvements in predictions of about 1%–6% (PC) and 1%–8% (HSS), when applied to SPI6, but regarding SPI12 only seven of the locations presented slight improvements of about 0.4%–1.8% (PC) and 0.7%–3% (HSS).

Keywords: 3-dimensional log-linear models; drought class transitions; *odds*; confidence intervals

1. Introduction

Drought is a natural temporary imbalance of water availability, consisting of a persistent lower-than-average precipitation, of uncertain frequency, duration and severity, and of unpredictable or difficult-to-predict occurrence, resulting in diminished water resource availability and carrying capacity of ecosystems [1]. The importance of early warning to water users for timely implementation of preparedness and mitigation measures is well known and has been widely addressed by several authors [1–3]. Developing prediction tools appropriate for the climatic and agricultural conditions prevailing in different drought-prone areas constitutes a research challenge. Drought prediction is a major concern for water managers, farmers and other water end-users because it constrains their decisions. Since droughts have a slow initiation, it is possible to release a timely prediction so that

measures and policies can be taken in order to mitigate the effects of the drought [3,4]. Short-term drought predictions, from one to three months, may be used to alert farmers and water managers about the initiation, continuation or end of a drought and about the need for preparedness measures before a drought is effectively installed or for a post-drought period. However, forecasting when a drought is likely initiating or to coming to an end is a difficult task.

Drought severity is usually identified through indices such as the Standardized Precipitation Index (SPI), the Palmer Drought Severity Index (PDSI) and the MedPDSI [5–7]. However, in the Interregional Workshop on Indices and Early Warning Systems for Drought 2009, several organizations, including the World Meteorological Organization (WMO) and the United States National Oceanic and Atmospheric Administration (NOAA), recommended that the SPI be used by all national meteorological and hydrological services around the world to characterize meteorological droughts as well as agricultural and hydrological droughts because the SPI is an index that is simple to understand, is easy to calculate and is statistically relevant and meaningful [8]. In fact, precipitation is the only required input parameter and it considers in its conception the different impacts on groundwater, reservoir storage, soil moisture, snowpack and stream-flow through the different time scales of computation [5,8]. The SPI is based on the probability of precipitation for any time scale. The probability of observed precipitation is then transformed into an index that supports assessing drought severity and may provide early warning of drought.

The precipitation occurrence and/or its inhibition leading to drought on different time and spatial scales is driven by atmospheric forcings which may range from the mesoscale (hundreds of km) up to the planetary scale (tens of thousands of km). The large-scale atmospheric state may roughly be described by a time-varying state vector filled with a few numbers of leading principal components of the sea-level pressure (SLP) field. That state vector either exhibits a transient behavior or persists near certain states, the so-called weather regimes (WRs) or atmospheric circulation patterns, which are detectable by cluster analysis [9]. Therefore, the projection or pattern correlation of the SLP field onto the main WRs acts as large-scale atmospheric circulation indices, which are useful indicators of the rainfall field. In particular, several large-scale indices of the Euro-Atlantic and Northern Hemisphere SLP field [10,11] are well correlated with the cumulated precipitation in certain target regions, namely Portugal [12]. We recall the main four Euro-Atlantic atmospheric WRs as: (1) the blocking regime, with a large anomalous high pressure over Scandinavia; (2) the zonal regime (positive phase of the North Atlantic Oscillation: NAO⁺), characterized by an intense zonal flow crossing the North Atlantic area, reinforcing the Icelandic low and the Azores' high pressure centers; (3) the Atlantic Ridge regime, exhibiting a positive anomaly over the North Atlantic and low pressure over northern Europe; and (4) the Greenland anticyclone pattern (negative phase of the North Atlantic Oscillation: NAO⁻), showing a strong positive pressure anomaly centered over western Greenland. Since some of the WRs display nearly symmetric anomalies, the corresponding projections of the SLP field are not independent. The overall main features of the Euro-Atlantic large-scale atmospheric field are then well captured by a set of large-scale indices: the North Atlantic Oscillation (NAO) index [13], the EAP (East-Atlantic Pattern) index, the SCAND (Scandinavian Pattern) index [14] and the East-Atlantic Western Russia (EAWR) index, all available at the National Centers for Environmental Prediction (NCEP) website. One of the main patterns governing wet and dry rainfall regimes in most of Europe is the NAO [14]. The NAO index is commonly given by the difference in normalized SLP anomalies between a southern node, located in continental Iberia or the Azores, and a northern node, usually in southwest Iceland [13,15]. Strong positive phases of the NAO (*i.e.*, NAO⁺) tend to be associated with above-average temperatures in the eastern United States and across northern Europe and below-average temperatures in Greenland and oftentimes across southern Europe and the Middle East. The NAO⁺ regime is also associated with above-average precipitation over northern Europe and Scandinavia in the winter, and below-average precipitation or drought over southern and central Europe, Mediterranean regions and the north of Africa. Opposite patterns of temperature and

precipitation anomalies are typically observed during strong negative phases of the NAO available at the National Centers for Environmental Prediction (NCEP) website.

Pires and Perdigão [16] have shown high levels of correlation between the NAO index and the SPI reaching the negative value -0.60 for the winter months for some locations in northern Portugal, which convert the NAO in an interesting tool for the improvement of drought predictions. The NAO influences on the precipitation regimes and droughts in Portugal and the Iberian Peninsula are also reported by other researchers [17,18]. Santos *et al.* [12] have shown that dry weather conditions prevail when the NAO index is positive (NAO⁺). The drought frequency in Portugal has been increasing as a consequence of a drying signal in the Mediterranean region attributable to a trend in the atmospheric circulation forcing, namely a decadal scale enhancement of the positive phase of the North Atlantic Oscillation [19].

Several statistical and physical-based techniques as well as the combination of both (hybrid techniques) have been proposed for the forecasting of droughts and the cumulated precipitation on a monthly basis. The state-of-the-art physical models used for weather and climate prediction such as that of the European Center for Medium Range Weather Forecasts (ECMWF) have been used for obtaining probabilistic ensemble-based forecasts up to six months in advance of the SPI worldwide on scales of three, six and 12 months [20]. Since the computational burden of those predictions is very high and they depend on the availability of a physical model, a reasonable alternative for the meteorological community started by developing simple statistical models of the monthly and seasonal cumulated precipitation [21,22]. Those models often apply multivariate statistical techniques such as the Canonical Correlation Analysis (CCA), robust multilinear regression, and Singular Spectrum Analysis (SSA), among others [23], and they rely on a set of previously well-chosen physical predictors that are able to capture the main boundary layer's forcing of the atmospheric dynamics (e.g., the sea surface temperature (SST), the snow cover and land moisture fields) and the intrinsic predictable features such as the internal (not externally forced) oscillations of the climatic system. In regard to hybrid predictions, we must refer to several techniques. On one hand, we have the mixing by Bayesian probabilistic averaging, either of different physical-based predictions [24] or of physical and statistical models [25]. On the other hand, we may use the optimal regression of physical precursors and dynamical forecasts of drought indices [26].

Hereby we will focus on statistical methods of drought prediction only. Combining the stochastic properties of the SPI with weather pattern indices such as NAO is a challenge for the short-term prediction of droughts by statistical methods. The stochastic properties of the SPI time series have been explored for analyzing and predicting drought class transitions in the Portuguese context [27–32].

The methodologies include regression analysis [33], time series modeling such as ARIMA and seasonal ARIMA [34,35], artificial neural network models (ANN) [36,37] and stochastic and probability models such as Markov chains [38–40], log-linear models [31,41] and others [42,43]. Also, hybrid models combining two techniques have been used, for instance wavelet transforms and neural networks [44], stochastic and neural network modeling [45], wavelet and fuzzy logic models [46], adaptive neuro-fuzzy inference [47] and data mining and ANFIS techniques [48]. Each methodology, independently of its complexity, has advantages and limitations. Mishra and Singh [49] recently reviewed and discussed the methodologies used so far for drought modeling.

Approaches to drought forecasting using drought indices associated with atmospheric-oceanic anomaly indices have been suggested for predictions on monthly and seasonal scales. Examples include the use of artificial neural networks and time series of drought indices additionally driving the NAO index [37], and the use of probabilistic models that result from evaluating conditional probabilities of future SPI classes with respect to current SPI and NAO classes [43].

Three-dimensional (3D) log-linear models allow modeling the state of a variable at time $t + 1$ knowing its state at time t and $t - 1$ [50]. Those models were used to predict SPI drought class transitions one and two months ahead, knowing the drought class of the last two months [31]. In this approach, log-linear models are fitted to 3D contingency tables of drought class transitions counts,

corresponding to two time-step transitions relative to the SPI drought classes at months $t - 1$, t and $t + 1$ obtained from categorical time series of SPI drought classes. Then, ratios of expected frequencies (*odds*) relative to the most probable transition for the next month and their confidence intervals are computed. This approach allows predictions with a leading time of two or more months and has shown potential to be improved, namely with the inclusion of new categories in the contingency tables. Recently, the introduction of a new variable representing the wet or the dry season of the year was tested in order to improve the predictions [41].

Considering the advances in drought predictions reviewed above and the reported NAO influence on precipitation and drought in Portugal, the objectives of this work consist of improving log-linear modeling of the SPI drought class transitions when driven by the negative or positive phases of the NAO index. This approach is an advance relative to the previous study [31] since it was based uniquely on the assessment of SPI drought classes. In the current study, long series of monthly precipitation of more than 100 years were used, which brings advantages in model-fitting and allows better estimates for the transition probabilities.

2. Materials and Methods

2.1. Data, SPI and NAO

The data used in this study consists of GPCC gridded precipitation with 1.0 degrees of spatial resolution and with 112 years length (1902–2014), for the 10 grid points located over mainland Portugal (Figure 1). The GPCC dataset is a gauge-based gridded monthly precipitation dataset for the global land surface, available in 2.5°, 1° and 0.5° spatial resolutions. The GPCC product used is the GPCC Precipitation Combined Full V6 and V4 Monitoring Data Product (1.0 × 1.0) available at the website of National Oceanic & Atmospheric Administration (NOAA)-Earth System Research Laboratory (ESRL).

Details regarding this dataset are available [51,52]. The GPCC dataset was used because the observation time series of monthly precipitation are somewhat short and have not been updated since 2006 while the adopted modeling approach benefits from using long and recent data to better parameterize and assess the model. The data set used in the current study was previously used [41]. Moreover, a recent study has shown that the temporal and spatial behaviors of the SPI computed on three-, six-, 12- and 24-month time scales with the GPCC data set compared well with those computed with observation data sets [53].

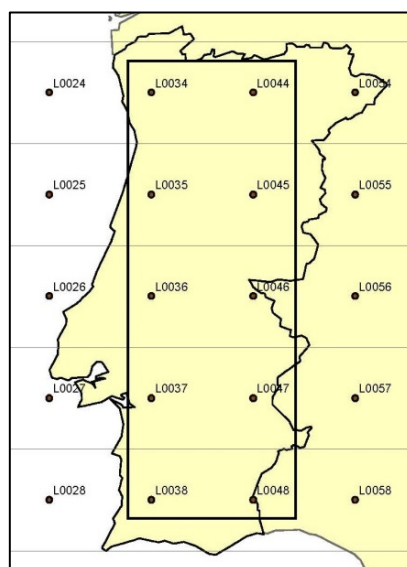


Figure 1. Selected grid locations in Portugal with a resolution of 1.0 × 1.0 degrees in longitude and latitude.

SPI values on a six-month (SPI6) and 12-month time scale (SPI12) were computed for the 10 precipitation time series referred above. The SPI12 is more appropriate to identify dry and wet periods of relatively long duration and relates better with impacts of drought on the hydrologic regimes [54]. Shorter time scales of six months or less are likely more useful to detect agricultural droughts, reflecting a better change of class instead of its persistence [54].

Categorical time series of monthly drought classes were computed based on Table 1, relative to both SPI6 and SPI12 time series; however, the severe and extremely severe drought classes in Table 1 were grouped because transitions referring to the extremely severe drought classes are much less frequent than those for other classes, therefore avoiding too many zeros in the contingency tables that may cause problems in the fitting.

Table 1. Drought class classification of SPI (modified from MCKEE *et al.* [55]).

Code	Drought Classes	SPI Values
1	Non-drought	$SPI \geq 0$
2	Near normal	$-1 < SPI < 0$
3	Moderate	$-1.5 < SPI \leq -1$
4	Severe/Extreme	$SPI \leq -1.5$

Monthly tabulated NAO indices, based on a Principal Component Approach of the Sea Level Pressure field and dating back to 1950, are available from the National Centers for Environmental Prediction (NCEP) Climate Prediction Center. However, in order to cover the full period of the precipitation data (1902–2014), we used an extended historical record (starting in 1864) of a station-based NAO index relying upon the difference of normalized SLP between Lisbon (Portugal) and Reykjavik (Iceland).

Before moving on to modeling, a correlation study was performed in order to find the lag between the NAO index and SPI time series that maximizes the correlation between them both. The Pearson correlation coefficient was computed between the monthly NAO index and the SPI6 and SPI12 time series for each grid location and a lag of five months for the SPI6 and 11 months for the SPI12 was found. In both cases, these lags indicate that the largest influence of NAO occurs near the starting month of the precipitation accumulation period for the SPI which is explained by the large memory of the NAO index and the contemporaneous (no lag) large correlation between monthly precipitation and the NAO index [16]. For the purposes of this modeling, when the NAO index for a given month is equal or greater than zero, then the NAO state in that month is positive, otherwise it is negative.

2.2. Modeling

For modeling purposes, the number of two-step monthly transitions between any SPI drought class was counted separately for the negative and positive NAO state to form two three-dimensional ($4 \times 4 \times 4$) contingency tables [50] with $N = 64$ cells each. These two contingency tables for NAO^- and NAO^+ have three categories: the drought class at month $t - 1$, t and $t + 1$ with four levels for each one (drought classes 1, 2, 3, and 4 defined in Table 1). Given the previously mentioned lag between the NAO and the SPI and considering that predictions focus on month $t + 1$, the NAO index was evaluated at month $t - 4$ or $t - 10$ which correspond to lags of 5 or 11 months for, respectively, the SPI6 and SPI12. Examples of these contingency tables are presented in Tables 2 and 3 for the SPI6 and SPI12. If the NAO state at month $t - 4$ ($t - 10$) was negative then the transition was counted for the table NAO^- , otherwise it was counted for the table NAO^+ .

Log-linear modeling input consists of the observed frequency n_{ijk} , $i, j, k = 1, \dots, 4$ reported in the contingency tables (e.g., Tables 2 and 3), which consist of the number of times that in a given month the drought class i was followed by the drought class j in the next month (one-step transitions) and then by the drought class k in the month after that (two-step transitions). The model computes the expected frequency m_{ijk} , $i, j, k = 1, \dots, 4$, i.e., the expected value $E(n_{ijk})$ of n_{ijk} , $i, j, k = 1, \dots, 4$.

Table 2. Three-dimensional contingency table for two consecutive transitions between drought classes of SPI6, computed for location L0034 in the northwest of Portugal (see Figure 1).

NAO ⁻	Drought Class Month $t + 1$				Drought Class Month $t + 1$				Drought Class Month $t + 1$				Drought Class Month $t + 1$			
	1				2				3				4			
drought class month $t - 1$	Drought class month t				Drought class month t				Drought class month t				Drought class month t			
	1	2	3	4	1	2	3	4	1	2	3	4	1	2	3	4
1	271	10	1	0	30	38	3	0	2	2	1	1	3	1	2	1
2	40	40	0	0	13	70	6	2	1	10	9	3	0	3	4	1
3	1	5	1	3	0	13	8	0	0	5	7	3	0	0	2	3
4	6	0	0	3	0	1	3	3	0	0	1	2	0	0	3	9

NAO ⁺	Drought class Month $t + 1$				Drought class Month $t + 1$				Drought class Month $t + 1$				Drought class Month $t + 1$			
	1				2				3				4			
drought class month $t - 1$	Drought class month t				Drought class month t				Drought class month t				Drought class month t			
	1	2	3	4	1	2	3	4	1	2	3	4	1	2	3	4
1	173	18	2	0	51	38	2	1	7	1	1	0	0	3	0	0
2	40	35	0	1	16	108	10	2	2	18	12	3	0	7	3	5
3	4	3	0	1	0	19	17	2	0	6	18	5	0	2	3	5
4	1	1	1	0	1	5	4	0	0	2	7	7	0	1	5	12

Table 3. Three-dimensional contingency table for two consecutive transitions between drought classes of SPI12, computed for location L0034 in the northwest of Portugal (see Figure 1).

NAO ⁻	Drought Class Month $t + 1$				Drought Class Month $t + 1$				Drought Class Month $t + 1$				Drought Class Month $t + 1$			
	1				2				3				4			
drought class month $t - 1$	Drought class month t				Drought class month t				Drought class month t				Drought class month t			
	1	2	3	4	1	2	3	4	1	2	3	4	1	2	3	4
1	308	4	0	0	19	18	0	0	0	2	0	0	0	0	0	0
2	21	19	0	0	4	134	4	0	0	10	6	0	0	1	1	1
3	1	2	0	0	0	8	3	0	0	0	19	1	0	0	7	7
4	1	0	0	0	0	2	2	1	0	1	5	5	0	0	4	28

NAO ⁺	Drought class Month $t + 1$				Drought class Month $t + 1$				Drought class Month $t + 1$				Drought class Month $t + 1$			
	1				2				3				4			
drought class month $t - 1$	Drought class month t				Drought class month t				Drought class month t				Drought class month t			
	1	2	3	4	1	2	3	4	1	2	3	4	1	2	3	4
1	244	9	0	0	30	29	0	0	1	0	1	0	0	1	0	0
2	24	23	0	0	10	152	8	2	0	17	10	1	0	2	3	0
3	2	2	1	0	0	14	8	1	0	1	22	5	0	0	7	10
4	0	0	2	1	0	2	2	2	0	1	4	9	0	0	2	21

Previous studies [31,56] have shown that the quasi-association (QA) log-linear models [50] were the ones that better fitted to similar two- and three-dimensional contingency tables; therefore, they were adopted in this study and are described in Appendix A.

When log-linear models are used, *odds* are computed. *Odds* are defined as ratios between expected transition frequencies. They indicate the proportion between the probabilities of transition to one class over another class and assume values from 0 to $+\infty$ [50]. Herein, an *odds* (defined with its confidence interval in Appendix A) represents the number of times that it is more, less, or equally probable that the occurrence of a drought class transition takes place over another, *i.e.*, they read that one month from now it is “*Odds_{kl|ij}*” times more, less, or equally probable, that a specific location will be in class *k* instead of class *l*, given that at month *t* (present) is in class *j*, and at month *t - 1* (past) was in class *i*. For the NAO at month *t - 5* (*t - 10*) is positive then we denote it by *Odds⁺_{kl|ij}*, otherwise by *Odds⁻_{kl|ij}*. For the logarithm of these *Odds*, asymptotic confidence intervals associated with a probability $1 - \alpha = 0.95$ were computed.

Odds confidence intervals, besides reflecting the sampling variability of the observed drought transitions internal to each time series, also indicate if a given odds is significantly different from 1. For a 5% significance level, if the confidence interval for an odds includes the value 1, then there is a 95% probability that the odds in fact equals 1, meaning that the drought transition from class i to class j to class k and the drought transition from class i to class j to class l are not significantly different. Otherwise, there is also a 95% probability that the odds is in fact larger (smaller) than 1, meaning that the first transition is significantly more (less) probable than the second. If the confidence interval of a given odds is too large then the reliability of the prediction is small.

For obtaining the most probable class transition for the month $t + 1$, the odds for the three closest class transitions, starting from the drought class at month t , are computed as well as their confidence intervals. The most probable transition is chosen. For instance, if the drought classes at month $t - 1$ and t are equal to 3 and 4, respectively, then $Odds_{34|34}$, $Odds_{24|34}$ and $Odds_{23|34}$ will be computed. If the values and respective confidence intervals obtained for those odds are, for instance, $Odds_{43|34} = 2.45[1.18, 3.89]$, $Odds_{42|34} = 5.35 [3.92, 8.62]$ and $Odds_{32|34} = 1.99 [0.76, 5.01]$, then class 4 is more probable than class 3 and much more probable than class 2, obviously because a jump from a class to another with a one-point difference is always more probable than that to a class with two or three points of difference. At last, class 3 is more probable than class 2, resulting in that class 4 is the most probable for the month $t + 1$, thus meaning maintenance of the previous class.

2.3. Model Performance

The model performance was assessed using the Heidke skill score (HSS) [23,57]. The HSS measures the fractional improvement of the forecast over a random prediction. The range of the HSS is $-\infty$ to 1. Negative values indicate that the chance forecast is better than the model prediction, HSS = 0 means no skill, while a perfect forecast obtains a HSS of 1. The computation of the HSS involves building the contingency table presented in Table 4 which is used in HSS and defined as follows:

$$HSS = \left(\sum_{i=1}^4 p_{ii} - \sum_{i=1}^4 p_i p'_i \right) / \left(1 - \sum_{i=1}^4 p_i p'_i \right) \tag{1}$$

where p_{ii} is the proportion of predictions that agreed with the observations for class i and p_{ik} is the proportion of events with predictions at class i and observed at class k with $i \neq k$, and p_i and p'_i are the marginal totals in Table 4. This approach was previously tested [41].

Table 4. Contingency table for the prediction of four drought classes for computing the Heidke skill score.

Drought Classes	Observed				Marginal total
	1	2	3	4	
predicted					
1	p_{11}	p_{12}	p_{13}	p_{14}	$p'_1 = \sum p_{1k}$
2	p_{21}	p_{22}	p_{23}	p_{24}	$p'_2 = \sum p_{2k}$
3	p_{31}	p_{32}	p_{33}	p_{34}	$p'_3 = \sum p_{3k}$
4	p_{41}	p_{42}	p_{43}	p_{44}	$p'_4 = \sum p_{4k}$
Marginal total	$p_1 = \sum p_{i1}$	$p_2 = \sum p_{i2}$	$p_3 = \sum p_{i3}$	$p_4 = \sum p_{i4}$	100%

The measure that gives the total number of agreements, called the proportion of corrects (PC), is easily obtained from Table 4, and is simply given by:

$$PC = \sum_{i=1}^4 p_{ii} \tag{2}$$

3. Results and Discussion

Both contingency tables for NAO^- and NAO^+ , either relative to the SPI6 (Table 2) or the SPI12 (Table 3), present higher frequency values for the transitions that imply the maintenance of the precedent drought classes and smaller frequencies for the transitions that imply the increase/decrease of the drought classes, particularly when changing by two or three values. As for previous studies [31,41], this maintenance trend results from the fact that droughts (of six- and 12-month temporal scales) install slowly, tend to remain for a relatively long time, and have a slow dissipation. These maintenance characteristics are less evident when using the SPI6 since it responds quickly to increases or decreases in the precipitation because the computation cumulative period is shorter than for SPI12. Data in Tables 2 and 3 show that NAO^- favors the transitions from drought class 1 to itself, *i.e.*, maintaining a non-drought condition, while the NAO^+ favors transitions from drought class 3 and 4 to themselves, although not significantly, *i.e.*, the maintenance of moderate and severe drought classes, particularly when considering the SPI6.

Tables 5 and 6 present results for four out of the 10 locations using, respectively, SPI6 and SPI12 data (L0035, L0038, L0045 and L0048). These tables allow us to compare the drought classes “OBS” when calculated from observed data and predicted with the log-linear modeling driven and not driven by NAO, respectively referred to as “predicted w/NAO” and “predicted”. The period selected for the comparison, October 2011 to February 2013, refers to a drought event, therefore including its initiation, development and dissipation. For each site, the observed SPI6 (SPI12) drought class at months $t - 1$ and t are presented, as well as the classes at month $t + 1$ “observed” and “predicted w/NAO” and “Predicted”. In addition, the NAO index values at month $t - 4$ ($t - 10$) are also presented. When two or three drought classes are equally probable, then the predicted drought class is identified as “1 or 2” or “2 or 3 or 4”, for instance, which means that probabilities for the transitions into classes 1 or 2 or into classes 2 or 3 or 4 are similar. The cells in Tables 5 and 6 are highlighted in grey when the predictions do not match the observations.

Results in Tables 5 and 6 show that the model performs very well in predicting the maintenance of the drought class, but generally does not perform well when a decrease or increase of the drought class category occurs which breaks with the drought class established in the preceding two months. Because of the negative correlation between the NAO index and precipitation in Iberia [12,16,17], the wet and less dry classes, *i.e.*, classes 1 and 2 (see Table 1), tend to occur when the NAO index is negative. However, with the log-linear model driven by NAO, some cases of class change could be predicted better, namely those in the negative NAO regime (NAO^-) (e.g., 13 February and 12 August for SPI6 in L0035), leading to wet conditions in western Iberia. That is because the sensitivity of precipitation to the NAO index is generally stronger in the wetter regimes, in accordance with the asymmetric correlations between NAO and SPI presented by Pires and Perdigão [16].

From comparing predictions relative to SPI6 (Table 5) with those of SPI12 (Table 6), it could be observed that the number of disagreements is large for SPI6. This behavior is likely due to the larger number of class changes in the case of SPI6, since this index denotes a shorter time span of the cumulated precipitation than SPI12 and therefore produces a quicker response to the variability of precipitation which results in more frequent changes of drought classes. Results for the other locations and for other drought events simulated have shown behaviors similar to those referred above.

Table 5. SPI6: comparison between observed (OBS) and predicted drought class transitions (“Predicted w/NAO” and “Predicted” for four locations during the period October 2011 to February 2013).

L0035				Drought Class at			Drought Class at Month $t + 1$			L0038			
Date	NAO	Month $t - 4$	Month $t - 1$	Month t	OBS	Predicted w/NAO	Predicted	date	Month $t - 1$	Month t	OBS	Predicted w/NAO	Predicted
October-2011	-1.58		3	3	2	2 or 3 or 4	2 or 3 or 4	October-2011	1	1	1	1	1
November-2011	-3.39		3	2	2	1 or 2	2	November-2011	1	1	2	1	1
December-2011	-0.18		2	2	3	2	2	December-2011	1	2	2	2	2
January-2012	2.97		2	3	4	2 or 3 or 4	2 or 3 or 4	January-2012	2	2	2	2	2
February-2012	1.45		3	4	4	4	4	February-2012	2	2	2	2	2
March-2012	0.74		4	4	4	4	4	March-2012	2	2	2	2	2
April-2012	3.2		4	4	4	4	4	April-2012	2	2	3	2	2
May-2012	2.05		4	4	4	4	4	May-2012	2	3	2	2 or 3	2 or 3
June-2012	1.28		4	4	3	4	4	June-2012	3	2	2	2	2
July-2012	1.78		4	3	2	2 or 3 or 4	2	July-2012	2	2	2	2	2
August-2012	-2.36		3	2	1	1 or 2	2	August-2012	2	2	2	2	2
September-2012	-0.83		2	1	1	1	1	September-2012	2	2	2	2	2
October-2012	-2.58		1	1	2	1	1	October-2012	2	2	1	2	2
November-2012	-1.31		1	2	2	1 or 2	2	November-2012	2	1	1	1	1
December-2012	-0.44		2	2	1	2	2	December-2012	1	1	1	1	1
January-2013	-1.44		2	1	2	1	1	January-2013	1	1	1	1	1
February-2013	-3.21		1	2	1	1 or 2	2	February-2013	1	1	1	1	1

L0045				Drought Class at			Drought Class at Month $t + 1$			L0048			
Date	NAO	Month $t - 4$	Month $t - 1$	Month t	OBS	Predicted w/NAO	Predicted	date	Month $t - 1$	Month t	OBS	Predicted w/NAO	Predicted
October-2011	-1.58		3	4	2	2 or 3 or 4	4	October-2011	1	1	1	1	1
November-2011	-3.39		4	2	3	2	2	November-2011	1	1	2	1	1
December-2011	-0.18		2	3	4	2 or 3 or 4	2 or 3 or 4	December-2011	1	2	2	2	2
January-2012	2.97		3	4	4	3 or 4	4	January-2012	2	2	3	2	2
February-2012	1.45		4	4	4	4	4	February-2012	2	3	3	2 or 3	2 or 3
March-2012	0.74		4	4	4	4	4	March-2012	3	3	3	2 or 3	2 or 3
April-2012	3.2		4	4	4	4	4	April-2012	3	3	4	2 or 3	2 or 3
May-2012	2.05		4	4	4	4	4	May-2012	3	4	4	3 or 4	4
June-2012	1.28		4	4	3	4	4	June-2012	4	4	4	3 or 4	4
July-2012	1.78		4	3	2	2 or 3 or 4	2 or 3	July-2012	4	4	2	3 or 4	4
August-2012	-2.36		3	2	1	1 or 2	2	August-2012	4	2	2	1 or 2	2
September-2012	-0.83		2	1	2	1	1	September-2012	2	2	2	2	2
October-2012	-2.58		1	2	1	1 or 2	2	October-2012	2	2	1	2	2
November-2012	-1.31		2	1	1	1	1	November-2012	2	1	1	1	1
December-2012	-0.44		1	1	1	1	1	December-2012	1	1	1	1	1
January-2013	-1.44		1	1	1	1	1	January-2013	1	1	2	1	1
February-2013	-3.21		1	1	1	1	1	February-2013	1	2	1	2	2

Table 6. SPI12: comparison between observed (OBS) and predicted drought class transitions (“Predicted w/NAO” and “Predicted” for four locations during the period October 2011 to February 2013).

L0035				NAO			Drought Class at			Drought Class at Month $t + 1$			L0038				Drought Class at			Drought Class at Month $t + 1$		
Date	Month $t - 10$	Month $t - 1$	Month t	OBS	Predicted w/NAO	Predicted	date	Month $t - 1$	Month t	OBS	Predicted w/NAO	Predicted	date	Month $t - 1$	Month t	OBS	Predicted w/NAO	Predicted				
October-2011	-4.62	2	2	2	2	2	October-2011	1	1	1	1	1	October-2011	1	1	1	1	1				
November-2011	-1.38	2	2	3	2	2	November-2011	1	1	1	1	1	November-2011	1	1	1	1	1				
December-2011	2.79	2	3	4	2 or 3 or 4	3	December-2011	1	1	1	1	1	December-2011	1	1	1	1	1				
January-2012	-0.44	3	4	4	4	3 or 4	January-2012	1	1	1	1	1	January-2012	1	1	1	1	1				
February-2012	2.39	4	4	4	4	4	February-2012	1	1	2	1	1	February-2012	1	1	2	1	1				
March-2012	1.08	4	4	4	4	4	March-2012	1	2	2	2	2	March-2012	1	2	2	2	2				
April-2012	-1.58	4	4	4	4	4	April-2012	2	2	2	2	2	April-2012	2	2	2	2	2				
May-2012	-3.39	4	4	4	4	4	May-2012	2	2	2	2	2	May-2012	2	2	2	2	2				
June-2012	-0.18	4	4	4	4	4	June-2012	2	2	2	2	2	June-2012	2	2	2	2	2				
July-2012	2.97	4	4	4	4	4	July-2012	2	2	2	2	2	July-2012	2	2	2	2	2				
August-2012	1.45	4	4	4	4	4	August-2012	2	2	2	2	2	August-2012	2	2	2	2	2				
September-2012	0.74	4	4	3	4	4	September-2012	2	2	2	2	2	September-2012	2	2	2	2	2				
October-2012	3.2	4	3	4	2 or 3 or 4	2 or 3 or 4	October-2012	2	2	2	2	2	October-2012	2	2	2	2	2				
November-2012	2.05	3	4	4	3 or 4	3 or 4	November-2012	2	2	2	2	2	November-2012	2	2	2	2	2				
December-2012	1.28	4	4	2	4	4	December-2012	2	2	2	2	2	December-2012	2	2	2	2	2				
January-2013	1.78	4	2	2	2	2	January-2013	2	2	1	2	2	January-2013	2	2	1	2	2				
February-2013	-2.36	2	2	1	2	2	February-2013	2	1	1	1	1	February-2013	2	1	1	1	1				

L0045				NAO			Drought Class at			Drought class at Month $t + 1$			L0048				Drought Class at			Drought Class at Month $t + 1$		
Date	Month $t - 10$	Month $t - 1$	Month t	OBS	Predicted w/NAO	Predicted	date	Month $t - 1$	Month t	OBS	Predicted w/NAO	Predicted	date	Month $t - 1$	Month t	OBS	Predicted w/NAO	Predicted				
October-2011	-4.62	2	2	2	2	2	October-2011	1	1	1	1	1	October-2011	1	1	1	1	1				
November-2011	-1.38	2	2	3	2	2	November-2011	1	1	1	1	1	November-2011	1	1	1	1	1				
December-2011	2.79	2	3	4	3	3	December-2011	1	1	1	1	1	December-2011	1	1	1	1	1				
January-2012	-0.44	3	4	4	4	3 or 4	January-2012	1	1	1	1	1	January-2012	1	1	1	1	1				
February-2012	2.39	4	4	4	4	4	February-2012	1	1	2	1	1	February-2012	1	1	2	1	1				
March-2012	1.08	4	4	4	4	4	March-2012	1	2	2	2	2	March-2012	1	2	2	2	2				
April-2012	-1.58	4	4	4	4	4	April-2012	2	2	3	2	2	April-2012	2	2	3	2	2				
May-2012	-3.39	4	4	4	4	4	May-2012	2	3	3	2 or 3	2 or 3	May-2012	2	3	3	2 or 3	2 or 3				
June-2012	-0.18	4	4	4	4	4	June-2012	3	3	3	3	3	June-2012	3	3	3	3	3				
July-2012	2.97	4	4	4	4	4	July-2012	3	3	3	3	3	July-2012	3	3	3	3	3				
August-2012	1.45	4	4	4	4	4	August-2012	3	3	3	3	3	August-2012	3	3	3	3	3				
September-2012	0.74	4	4	4	4	4	September-2012	3	3	3	3	3	September-2012	3	3	3	3	3				
October-2012	3.2	4	4	4	4	4	October-2012	3	3	3	3	3	October-2012	3	3	3	3	3				
November-2012	2.05	4	4	3	4	4	November-2012	3	3	2	3	3	November-2012	3	3	2	3	3				
December-2012	1.28	4	3	2	2 or 3 or 4	2 or 3 or 4	December-2012	3	2	2	2	2	December-2012	3	2	2	2	2				
January-2013	1.78	3	2	2	2	2	January-2013	2	2	2	2	2	January-2013	2	2	2	2	2				
February-2013	-2.36	2	2	1	2	2	February-2013	2	2	1	2	2	February-2013	2	2	1	2	2				

In order to have a true picture of the performance of the model driven by the NAO compared to the model that is not driven by the NAO, the proportion of corrects (PC) and the Heidke skill score (HSS) were computed for the entire period of the time series. PC and HSS results are shown in Tables 7 and 8 respectively, for the SPI6 and the SPI12. These results show that improvements in the predictions occur when using the model with the NAO driven compared to the model without that driven: relative to SPI6, improvements of the PC score range from 1% to 5.6%, averaging 3%, while the HSS shows improvements ranging from 1.3% to 8.5% with an average of 4.5% (Table 7); for SPI12, three locations did not show any improvement when using modeling driven by the NAO, while the other seven locations' improvements were quite small, ranging from 0.4% to 2% for PC and 0.7% to 3.2% for HSS (Table 8).

Table 7. SPI6: results for the proportion of corrects (PC) and the Heidke skill score (HSS) for the model with the NAO driven (Model w/NAO) and the model without the NAO driven (Model) and the difference between both.

SPI6	PC			HSS		
	Model w/NAO	Model	Difference	Model w/NAO	Model	Difference
L0034	75.95%	72.17%	3.78%	59.98%	53.99%	5.99%
L0035	77.37%	74.18%	3.19%	62.27%	57.41%	4.86%
L0036	73.94%	70.83%	3.10%	56.96%	52.08%	4.88%
L0037	75.51%	72.62%	2.89%	58.40%	54.74%	3.67%
L0038	75.13%	74.10%	1.03%	58.85%	57.51%	1.34%
L0044	76.55%	70.91%	5.64%	61.02%	52.49%	8.53%
L0045	77.07%	73.74%	3.34%	61.90%	56.97%	4.93%
L0046	74.24%	73.29%	0.95%	57.50%	55.80%	1.69%
L0047	75.36%	71.95%	3.41%	59.06%	53.69%	5.36%
L0048	76.63%	73.81%	2.82%	61.27%	57.22%	4.05%

The application of the log-linear modeling driven by the NAO produces larger improvements of predictions when applied to the SPI6 compared to SPI12, which is likely due to the fact that the correlation between the NAO index (always taken as the monthly value at the beginning of the precipitation accumulation period—PAP) and SPI6 is larger than that with SPI12. This is quite understandable due to the decreasing lagged cross-correlation function between a monthly NAO index value and the forthcoming monthly precipitation values and due to the fact that the PAP of SPI12 is larger compared to that of SPI6. This may also be explained by the slow response to changes in precipitation of SPI12, which produces fewer changes in drought classes compared with SPI6.

The overall modeling performances are good: PC scores ranged from 73.9% to 77.3% and 82.6% to 85.5% when using SPI6 and SPI12, respectively, while HSS scores ranged from 57.0% to 62.3% and 72.3% to 76.4% (HSS) for SPI6 and SPI12, respectively. Those scores normally decrease with the forecast lag (a single month here). Much of the scores are explained by the time overlapping between the SPI precipitation accumulation period of the forecast class and those used as predictors (the previous two months), in our case: five out of six months in SPI6 and 11 out of 12 months in SPI12.

Table 8. SPI12: results for the proportion of corrects (PC) and the Heidke skill score (HSS) for the model with the NAO driven (Model w/NAO) and the model without the NAO driven (Model) and the difference between both.

SPI12	PC			HSS		
	Model w/NAO	Model	Difference	Model w/NAO	Model	Difference
L0034	83.90%	83.11%	0.79%	73.84%	72.62%	1.22%
L0035	84.04%	82.96%	1.08%	73.99%	72.06%	1.93%
L0036	83.30%	84.15%	−0.85%	72.86%	74.56%	−1.70%
L0037	82.55%	82.14%	0.41%	72.27%	71.56%	0.71%
L0038	85.47%	83.63%	1.84%	76.40%	73.52%	2.88%
L0044	84.27%	82.22%	2.05%	74.08%	70.89%	3.19%
L0045	84.72%	83.78%	0.94%	75.08%	73.52%	1.56%
L0046	84.04%	83.26%	0.78%	74.10%	72.77%	1.33%
L0047	82.62%	83.18%	−0.56%	72.33%	73.10%	−0.77%
L0048	83.07%	83.18%	−0.11%	72.71%	72.83%	−0.12%

The better performances obtained with the modeling application of SPI12 are likely related to the less frequent change of drought classes with SPI12, which favors capturing the behavior of changes in drought classes in the preceding months. Indeed, the number of changes in drought class is almost double that of SPI6 when compared with the SPI12. These numbers were computed and are presented in Table 9, jointly with other relevant information explained later in the next paragraph. For both SPI12 and SPI6, when the maintenance in a given class breaks due to an increase or decrease of rainfall, the modeling fails in predicting the future drought class. Nevertheless, the maintenance in a given class is well captured by the model.

Table 9. Percentage of correct class change predictions relative to the total number of cases in which the observed drought class at month $t + 1$ differs from the drought class in the previous month for the model with and without NAO, as well as the total number of class changes for the SPI6 and SPI12.

SPI6	L0034	L0035	L0036	L0037	L0038	L0044	L0045	L0046	L0047	L0048	Average
Model w/NAO	16.2	17.1	15.8	17.3	25.8	20.0	20.1	13.2	17.9	21.9	18.5
Model	11.3	11.0	14	13.4	17.3	7.4	12.1	12.9	13.6	14.5	12.8
Difference	4.9	6.1	1.8	3.9	8.5	12.6	8	0.3	4.3	7.4	5.8
Nr. class changes	421	403	443	421	438	404	422	432	431	421	423.6
SPI12	L0034	L0035	L0036	L0037	L0038	L0044	L0045	L0046	L0047	L0048	Average
Model w/NAO	10.4	15.0	8.5	6.5	17.2	11.4	15.2	19.3	7.3	6.2	11.7
Model	5.6	10.1	14.1	3.2	9.8	2.4	11.7	16.7	9.7	6.2	9.0
Difference	4.8	4.9	−5.6	3.3	7.4	9	3.5	2.6	−2.4	0	2.8
Nr. class changes	249	267	248	248	244	246	256	270	278	241	254.7

The percentage of correct predictions when a drought class change occurs relative to the total number of cases when the observed drought class at month $t + 1$ differs from the drought class in the previous month was computed. Results are presented in Table 9 and refer to the entire time series length regarding the NAO driven predictions, the predictions without the NAO driven and their difference. These results show that the percentage of “predictions w/NAO” that agree with the observed class when there was a class change ranges from 13.2% to 25.8% with an average of 18.5% for SPI6 and from 6.2% to 19.2% with an average of 11.5% for SPI12. Relative to the model with the NAO forcing, those percentages are indeed slightly higher, showing an increase in the percentage of corrects ranging from 0.3% to 12.6% with an average of 5.8% for SPI6. For SPI12, this increase occurs in seven locations ranging from 2.6% to 9%, showing consistency with Table 8 where the same remaining three locations did not present improvement in the predictions.

These results show that log-linear modeling applied to both SPI6 and SPI12 actually cannot adequately predict the correct class change when there is a break relative to the drought class established in the previous two months. Those are cases where the rainfall regime during the two last

months of the SPI precipitation period was totally different from the remaining ones. Maybe in these cases, though not *a priori* detectable, the lag between the NAO index and the SPI should be smaller in respect to the NAO⁻ conditioned probability transition matrices. However, the fact that some of these cases can be predicted indicates that it may be possible to further use the model and particularly improve the way it is driven by NAO, namely using shorter time lags between NAO and SPI despite the fact that these do not correspond to the best correlation results. Another modification in modeling consists in considering three NAO states—very negative, around zero and very positive—instead of two, negative and positive, as used in this study. In fact, under the influence of a very negative (positive) NAO state, the model may be forced to strongly favor a decrease (increase) of drought class. The middle state, near zero, should not favor any transition.

4. Conclusions

This paper has contributed to the improvement of the log-linear forecasting models of drought class transitions [31,32] by conceiving a general method which includes the dependence of past drought SPI classes on a set of mutually exclusive weather regimes or large-scale mid-latitude atmospheric patterns. Its usefulness relies on the influence of Euro-Atlantic WRs, with particular relevance of the North Atlantic Oscillation on the large-scale European rainfall field [13,16,18], and on target regions such as Portugal and the Iberian Peninsula [12,17], through the influence of WRs on the meridional shifting of the polar front and storm-tracks [13]. Despite the availability either of statistical forecasting models (e.g., those based on multivariate linear regression) of the cumulated quantitative precipitation [21,22], which could eventually be converted into SPI classes, or of stochastic continuous models of the drought indices [34–37], the log-linear modeling assigns the SPI classes' forecasted probabilities, which might potentially be useful as input into economic value decision models. Moreover, the log-linear models have the advantage of choosing the SPI partition set in a suited manner for discriminating different levels of drought severity (negative SPI values) or in alternative, different levels of rain exceedances and floods (positive SPI values). Another relevant issue is the fact that drought forecasting has essentially the same nature of the seasonal-to-annual weather forecasting problem, *i.e.*, they are both probabilistic in essence due to the determinist chaotic nature of atmospheric dynamics. They have been evaluated, though not still operationally by the ECMWF integrated seasonal forecasted system [20], and therefore, simple probabilistic log-linear models, such as that designed in the paper, may capture some signals of the probability forecasts of drought.

In particular, for the developed model, the log-linear modeling of SPI drought class transitions driven by the NAO brought some improvements in the predictions when applied to SPI6 in comparison to the model not driven by the NAO. The improvement is relatively modest since much of the NAO influence on SPI is already implicit, even in a transition model without the explicit NAO forcing. That is because of the tight correlation of about -0.60 between monthly precipitation and the NAO index in western Iberia [16]. Regarding the application to SPI12, it cannot be concluded that a real improvement in predictions exists since only seven of the locations presented slight improvements.

The overall performances of the log-linear modeling are good, so it can be concluded that the log-linear modeling, when applied to SPI6 and SPI12, performs well in predicting the drought class one month ahead while knowing the drought classes of the two previous months, although it fails in predicting many transitions to a drought class that is different than the drought classes in the previous two months; nevertheless, it captures the maintenance of the drought class very well. With the use of the model driven by the NAO, some transitions of class can be correctly predicted, namely those under the influence of negative NAO. On those events under the negative NAO phase, the class predictions tend to be shifted to wetter classes as compared to the predictions without the explicit forcing of NAO. Conversely and consistently, a strengthening or maintenance of the drought became more probable in the NAO-driven predictions throughout the subset of events under the positive phase of the NAO. As a whole, the skill of drought classes' forecasts is consistent with that of linear statistical schemes of the continuous quantitative precipitation referred to in the introduction.

Overall, results show that the log-linear approach driven by NAO may be used with drought monitoring and forecasting since it provides useful information to water managers and users, helping them in their decisions to mitigate drought. Future research will focus on considering shorter time lags between SPI and NAO indices, using a NAO index with three states, as well as including other weather regime indices (e.g., NAO, EAP, SCAND and EAWR [13,14]) into the log-linear modeling or a Markov chain approach. Another approach could consider time averages (e.g., three or six months of averaging) other than the monthly averages of the NAO index used here.

Acknowledgments: This work was partially supported by the Fundação para a Ciência e a Tecnologia (Portuguese Foundation for Science and Technology) through the project PTDC/GEO-MET/3476/2012 on “Predictability assessment and hybridization of seasonal drought forecasts in western Europe” and through the project UID/MAT/00297/2013 (Centro de Matemática e Aplicações).

Author Contributions: The Elsa Moreira performed modeling, and wrote the paper in collaboration with the other authors. Carlos Pires led the NAO approaches and, together with Luís Pereira, contributed to writing and to the review of the study.

Conflicts of Interest: The authors declare no conflict of interest.

Appendix A—Technical Details on the Log-Linear Modeling and Odds

The observed frequency n_{ijk} , $i, j, k = 1, \dots, 4$ reported in the contingency tables consists of the number of times that, in a given month, the drought class i was followed by the drought class j in the next month, and then by the drought class k in the month after that (two-step transitions). Denoted by m_{ijk} , $i, j, k = 1, \dots, 4$, the expected frequency, which is the expected value $E(n_{ijk})$ of n_{ijk} , $i, j, k = 1, \dots, 4$, of the QA log-linear model is given by:

$$\log m_{ijk} = \lambda + \lambda_i^a + \lambda_j^b + \lambda_k^c + \beta ij + \alpha ik + \eta jk + \tau ijk + \delta_{1i}I(i = j) + \delta_{2i}I(i = k) + \delta_{3j}I(j = k) + \delta_{4i}I(i = j = k) \quad (A1)$$

where:

- λ is the constant parameter also designated by grand mean;
- λ_i^a, λ_j^b and λ_k^c are the effects of the i, j and k levels of category A, B and C, respectively (drought class at month $t - 1, t$ and $t + 1$), with $i, j, k = 1, \dots, 4$;
- β, α, η and τ are the linear association parameters between the categories;
- $\delta_{1i}, \delta_{2i}, \delta_{4i}$, are the parameters associated with the i -th diagonal element of category A; δ_{3j} is associated with the j -th diagonal element of category B;
- I takes the value 1 when the condition holds and the value 0 otherwise.

The expected frequencies m_{ijk} represent the expected number of two transitions between the drought classes i, j , and k in two consecutive months during the study period. The ratios of expected frequencies are the *odds*, which indicate the proportion between the probabilities of occurrence for two different events and assume values from 0 to $+\infty$ [50]. *Odds* is defined as:

$$Odds_{kl|ij} = m_{ijk}/m_{ijl}, \quad k \neq l, \quad \text{and } i, j, k, l = 1, \dots, 4 \quad (A2)$$

For the logarithm of these *Odds*, asymptotic confidence intervals associated with a probability $1 - \alpha$ can be computed, which are given by:

$$\left[\text{Log } Odds_{kl|ij} - q_{1-\alpha/2} \sqrt{V(\text{Log } Odds_{kl|ij})}, \text{Log } Odds_{kl|ij} + q_{1-\alpha/2} \sqrt{V(\text{Log } Odds_{kl|ij})} \right] \quad (A3)$$

where $q_{1-\alpha/2}$ is the $1 - \alpha/2$ quantile of a standard normal variable and $V(\text{Log } Odds_{kl|ij})$ is the variance of the $\text{Log } Odds_{kl|ij}$. The estimates of the *odds* and corresponding asymptotic confidence intervals are obtained by exponentiation of the respective interval borders for the logarithm of the *odds*.

The QA log-linear models allow for linear-by-linear association of the main diagonal of the contingency tables and are adequate to fit tables where the number of levels per category is the

same and have ordered categories, resulting from a pairwise comparison of dependent samples, which is the case [39]. In adjusting these models, it is assumed that the n_{ijk} , $i, j, k = 1, \dots, 4$ are values taken by independent Poisson distributed variables and the parameter estimators $\hat{\lambda}, \hat{\lambda}_i^a, \hat{\lambda}_j^b, \hat{\lambda}_k^c, \hat{\beta}, \delta_{ij}$ and $\hat{m}_{i,j,h}$, $h, j = 1, \dots, 4$, obtained using the maximum likelihood method, are asymptotically normally distributed [50]. The assumption of independency of n_{ijk} , $i, j, k = 1, \dots, 4$ could be considered because transitions between drought classes in successive months mainly depend on the amount of precipitation occurring in those months, not on transitions in previous months [40].

Not all the parameters in the model are linearly independent because of the constraint:

$$\sum_{i=1}^4 \lambda_i^a = \sum_{j=1}^4 \lambda_j^b = \sum_{k=1}^4 \lambda_k^c \tag{A4}$$

which is required in this kind of modeling in order to make the parameters identifiable [50]. As a result, it was assumed $\lambda_1^a = \lambda_1^b = \lambda_1^c = 0$, thus simplifying the model as in previous studies [31].

To ease the computations, a matrix notation may be used. The linearly independent parameters in the model are 30:

$$(\lambda, \lambda_2^a, \lambda_3^a, \lambda_4^a, \lambda_2^b, \lambda_3^b, \lambda_4^b, \lambda_2^c, \lambda_3^c, \lambda_4^c, \alpha, \beta, \eta, \tau, \delta_{11}, \delta_{12}, \delta_{13}, \delta_{14}, \delta_{21}, \delta_{22}, \delta_{23}, \delta_{24}, \delta_{31}, \delta_{32}, \delta_{33}, \delta_{34}, \delta_{41}, \delta_{42}, \delta_{43}, \delta_{44})$$

and they constitute the parameter vector θ , with components $\theta_1, \dots, \theta_{30}$, where, for instance, $\theta_2 = \lambda_2^a$. The corresponding maximum likelihood estimators of the parameters will constitute the vector $\hat{\theta}$. Let, n and m be, respectively, the vectors of observed frequencies and expected frequencies all ordered according to the index $s = 16i + 4j + k - 20$. This ordering is required because the QA log-linear models have to be rewritten in a matrix notation for computational purposes. The model matrix X , containing known constants, is a 64×30 matrix derived from Equation (A1). This matrix X is the same for all contingency tables because it relates to the QA log-linear model and does not depend on the data set. The QA log-linear model in matrix notation is then:

$$\mathbf{Log}(\mathbf{m}) = X\theta \tag{A5}$$

Considering that a rather long time span was used [50], it may be assumed that the vector $\hat{\theta}$ of the estimates has a normal distribution with mean value θ and with the variance-covariance matrix:

$$\mathbf{COV} = (X^T \mathbf{D}(\hat{\mathbf{m}}) X)^{-1} \tag{A6}$$

where $\mathbf{D}(\hat{\mathbf{m}})$ is the diagonal matrix whose principal elements are the expected frequency estimates and -1 indicates the inverse of the matrix. Moreover, the vector $\hat{\theta}$ is independent from the residual deviance

$$G^2 = 2 \sum_i \sum_j \sum_k n_{ijk} \text{Log} \left(n_{ijk} / m_{ijk} \right) \tag{A7}$$

working as the measure for the goodness of fit of the log-linear model. G^2 is asymptotically distributed as a central Chi-Square with four degrees of freedom, since there are 16 cells in the contingency tables and 12 linearly independent parameters to be adjusted [50]. As a result, to validate the adjustment of the model, the Chi-Square test with statistic G^2 may be used [50,58]. The null hypothesis that the model fits well and the data is not rejected for those models having a residual deviance not exceeding the Chi-Square quantile for a probability $1 - \alpha = 0.95$ and the corresponding degrees of freedom, *i.e.*, the models presenting a test p -value exceeding the chosen significance level are considered well fitted.

For obtaining the confidence intervals for the *odds*, we need to compute $V(\text{Log Odds}_{kl|ij})$. So, let us consider the row vectors of the matrix \mathbf{X} designated by \mathbf{x}_s with $s = 1, \dots, 64$. From Equation (A5), the logarithms of the expected frequencies are given by:

$$\hat{z}_s = \mathbf{x}_s^T \hat{\boldsymbol{\theta}}, s = 1, \dots, 64 \quad (\text{A8})$$

where T stands for transpose. Those values are also normally distributed with variance:

$$V(\hat{z}_s) = \mathbf{x}_s^T (\mathbf{X}^T \mathbf{D}(\hat{\mathbf{m}}) \mathbf{X}) \mathbf{x}_s, s = 1, \dots, 64 \quad (\text{A9})$$

For large samples, the $\text{Odds}_{kl|ij}$ have asymptotic normal distribution and the logarithmic transform $\text{Log Odds}_{kl|ij} = \text{Log } E_{ijk} - \text{Log } E_{ijl}$ converges more rapidly to a normal distribution. Thus,

$$\text{Log Odds}_{kl|ij} = \hat{z}_{s1} - \hat{z}_{s2} \quad (\text{A10})$$

where $s1$ and $s2$ correspond to the class transitions ijk and ijl , respectively, which is sorted according to the index s . So the variance for the Log Odds to be used in Equation (A3) can be easily computed as follows:

$$V(\text{Log Odds}_{kl|ij}) = (\mathbf{x}_{s1} - \mathbf{x}_{s2})^T (\mathbf{X}^T \mathbf{D}(\hat{\mathbf{m}}) \mathbf{X}) (\mathbf{x}_{s1} - \mathbf{x}_{s2}) \quad (\text{A11})$$

References

- Pereira, L.S.; Cordery, I.; Iacovides, I. Coping with Water Scarcity. In *Addressing the Challenges*; Springer: Berlin, Germany, 2009; p. 382.
- Wilhite, D.A.; Sivakumar, M.V.K., Wood, D.A., Eds.; Early Warning Systems for Drought Preparedness and Drought Management. In Proceedings of an Expert Group Meeting, Lisbon, Portugal, 5–7 September 2000; World Meteorological Organization: Geneva, Switzerland, 2000; p. 208.
- Pozzi, W.; Sheffield, J.; Stefanski, R.; Cripe, D.; Pulwarty, R.; Vogt, J.V.; Heim, R.R., Jr.; Brewer, M.J.; Svoboda, M.; Westerhoff, R.; *et al.* Toward global drought early warning capability: Expanding international cooperation for the development of a framework for monitoring and forecasting. *Am. Meteorol. Soc.* **2013**, *94*, 776–785. [[CrossRef](#)]
- Pulwarty, R.S.; Sivakumar, M.V.K. Information systems in a changing climate: Early warnings and drought risk management. *Weather Clim. Extremes* **2014**, *3*, 14–21. [[CrossRef](#)]
- McKee, T.B.; Doesken, N.J.; Kleist, J. The relationship of drought frequency and duration to time scales. In Proceedings of 8th Conference on Applied Climatology, California, CA, USA, 17–22 January 1993; pp. 179–184.
- Palmer, W.C. *Meteorological Drought*; US Department of Commerce: Washington, DC, USA, 1965.
- Paulo, A.A.; Rosa, R.D.; Pereira, L.S. Climate trends and behavior of drought indices based on precipitation and evapotranspiration in Portugal. *Nat. Hazards Earth Syst. Sci.* **2012**, *12*, 1481–1491. [[CrossRef](#)]
- World Meteorological Organization. *Standardized Precipitation Index User Guide*; WMO: Geneva, Switzerland, 2012. Available online: http://www.wamis.org/agm/pubs/SPI/WMO_1090_EN.pdf (accessed on 8 December 2015).
- Vautard, R. Multiple weather regimes over the North Atlantic: Analysis of precursors and successors. *Mon. Weather Rev.* **1990**, *118*, 2056–2081. [[CrossRef](#)]
- Michelangeli, P.A.; Vautard, R.; Legras, B. Weather regimes: Recurrence and quasi stationarity. *J. Atmos. Sci.* **1995**, *52*, 1237–1256. [[CrossRef](#)]
- Cassou, C.; Terray, L.; Hurrell, J.; Deser, C. North Atlantic climate regimes: Spatial asymmetry, stationarity with time, and oceanic forcing. *J. Clim.* **2004**, *17*, 1055–1068. [[CrossRef](#)]
- Santos, J.A.; Corte-Real, J.; Leite, S.M. Weather regimes and their connection to the winter rainfall in Portugal. *Int. J. Climatol.* **2005**, *25*, 33–50. [[CrossRef](#)]
- Hurrell, J.W. Decadal trends in the North Atlantic Oscillation: Regional temperatures and precipitation. *Science* **1995**, *269*, 676–679. [[CrossRef](#)] [[PubMed](#)]

14. Barnston, A.G.; Livezey, R.E. Classification, seasonality and persistence of low-frequency atmospheric circulation patterns. *Mon. Weather Rev.* **1987**, *115*, 1825–1850. [[CrossRef](#)]
15. Jones, P.D.; Jonsson, T.; Wheeler, D. Extension to the North Atlantic oscillation using early instrumental pressure observations from Gibraltar and south-west Iceland. *Int. J. Climatol.* **1997**, *17*, 1433–1450. [[CrossRef](#)]
16. Pires, C.A.; Perdigão, R. Non-Gaussianity and asymmetry of the winter monthly precipitation estimation from the NAO. *Mon. Weather Rev.* **2007**, *135*, 430–448. [[CrossRef](#)]
17. Trigo, R.M.; Pozo-Vázquez, D.; Osborn, T.J.; Castro-Díez, Y.; Gámiz-Fortis, S.; Esteban-Parra, M.J. North Atlantic Oscillation influence on precipitation, river flow and water resources in the Iberian Peninsula. *Int. J. Climatol.* **2004**, *24*, 925–944. [[CrossRef](#)]
18. López-Moreno, J.I.; Vicente-Serrano, S.M. Positive and negative phases of the wintertime North Atlantic Oscillation and drought occurrence over Europe: A multitemporal-scale approach. *J. Clim.* **2008**, *21*, 1220–1243. [[CrossRef](#)]
19. Hoerling, M.; Eischeid, J.; Perlwitz, J.; Quan, X.; Zhang, T.; Pegion, P. On the Increased Frequency of Mediterranean Drought. *J. Clim.* **2012**, *25*, 2146–2161. [[CrossRef](#)]
20. Dutra, E.; Pozzi, W.; Wetterhall, F.; Di Giuseppe, F.; Magnusson, L.; Naumann, G.; Barbosa, P.; Vogt, J.; Pappenberger, F. Global meteorological drought—Part 2: Seasonal forecasts. *Hydrol. Earth Syst. Sci.* **2014**, *18*, 2669–2678. [[CrossRef](#)]
21. Barnston, A.G. Linear statistical short-term climate predictive skill in the Northern Hemisphere. *J. Clim.* **1994**, *7*, 1513–1564. [[CrossRef](#)]
22. Coelho, C.A.S.; Stephenson, D.B.; Balmaseda, M.; Doblas-Reyes, F.J.; van Oldenborgh, G.J. Towards an integrated seasonal forecasting system for South America. *J. Clim.* **2006**, *19*, 3704–3721. [[CrossRef](#)]
23. Wilks, D.S. *Statistical Methods in the Atmospheric Sciences*, 3rd ed.; Academic Press: Cambridge, MA, USA, 2011; p. 704.
24. Wang, Q.J.; Schepen, A.; Robertson, D.E. Merging Seasonal Rainfall Forecasts from Multiple Statistical Models through Bayesian Model Averaging. *J. Clim.* **2012**, *25*, 5524–5537. [[CrossRef](#)]
25. Stephenson, D.B.; Coelho, C.A.S.; Doblas-Reyes, F.J.; Balmaseda, M. Forecast Assimilation: A Unified Framework for the Combination of Multi-Model Weather and Climate Predictions. *Tellus* **2005**, *57A*, 253–264. [[CrossRef](#)]
26. Ribeiro, A.; Pires, C.A. Seasonal drought predictability in Portugal using statistical-dynamical techniques. *J. Phys. Chem. Earth* **2015**, *17*, 1701–1717. [[CrossRef](#)]
27. Martins, D.S.; Raziei, T.; Paulo, A.A.; Pereira, L.S. Spatial and temporal variability of precipitation and drought in Portugal. *Nat. Hazards Earth Syst. Sci.* **2012**, *12*, 1493–1501. [[CrossRef](#)]
28. Moreira, E.; Mexia, J.T.; Pereira, L.S. Assessing homogeneous regions relative to drought class transitions using an ANOVA-like inference. Application to Alentejo, Portugal. *Stoch. Environ. Res. Risk Assess.* **2012**, *27*, 183–193. [[CrossRef](#)]
29. Moreira, E.E.; Mexia, J.T.; Pereira, L.S. Are drought occurrence and severity aggravating? A study on SPI drought class transitions using log-linear models and ANOVA-like inference. *Hydrol. Earth Syst. Sci.* **2012**, *16*, 3011–3028. [[CrossRef](#)]
30. Santos, J.F.; Pulido-Calvo, I.; Portela, M. Spatial and temporal variability of droughts in Portugal. *Water Resour. Res.* **2010**, *46*, W03503. [[CrossRef](#)]
31. Moreira, E.E.; Coelho, C.A.; Paulo, A.A.; Pereira, L.S.; Mexia, J.T. SPI-based drought category prediction using log-linear models. *J. Hydrol.* **2008**, *354*, 116–130. [[CrossRef](#)]
32. Paulo, A.A.; Pereira, L.S. Stochastic prediction of drought class transitions. *Water Resour. Manag.* **2008**, *22*, 1277–1296. [[CrossRef](#)]
33. Liu, W.T.; Negron-Juarez, R.I. ENSO drought onset prediction in northeast Brazil using NDVI. *Int. J. Remote Sens.* **2001**, *22*, 3483–3501. [[CrossRef](#)]
34. Han, P.; Wang, P.; Zhang, S.; Zhu, D. Drought forecasting based on the remote sensing data using ARIMA models. *Math. Comput. Model.* **2010**, *51*, 1398–1403. [[CrossRef](#)]
35. Mishra, A.K.; Desai, V. Drought forecasting using stochastic models. *Stoch. Environ. Res. Risk Assess.* **2005**, *19*, 326–339. [[CrossRef](#)]
36. Mishra, A.; Desai, V. Drought forecasting using feed-forward recursive neural network. *Ecol. Model.* **2006**, *198*, 127–138. [[CrossRef](#)]

37. Morid, S.; Smakhtin, V.; Bagherzadeh, K. Drought forecasting using artificial neural networks and time series of drought indices. *Int. J. Climatol.* **2007**, *27*, 2103–2111. [[CrossRef](#)]
38. Lohani, V.K.; Loganathan, G.V. An early warning system for drought management using the Palmer Drought Index. *J. Am. Water Resour. Assoc.* **1997**, *33*, 1375–1386. [[CrossRef](#)]
39. Lohani, V.K.; Loganathan, G.V.; Mostaghimi, S. Long-term analysis and short-term forecasting of dry spells by Palmer Drought Severity Index. *Hydrol. Res.* **1998**, *29*, 21–40.
40. Paulo, A.A.; Pereira, L.S. Prediction of SPI drought class transitions using Markov chains. *Water Resour. Manag.* **2007**, *21*, 1813–1827. [[CrossRef](#)]
41. Moreira, E.E. SPI drought class prediction using log-linear models applied to wet and dry seasons. *Phys. Chem. Earth* **2015**. in press. [[CrossRef](#)]
42. Cancelliere, A.; Di Mauro, G.; Bonaccorso, B.; Rossi, G. Drought forecasting using the Standardized Precipitation Index. *Water Resour. Manag.* **2007**, *21*, 801–819. [[CrossRef](#)]
43. Bonaccorso, B.; Cancelliere, A.; Rossi, G. Probabilistic forecasting of drought class transitions in Sicily (Italy) using Standardized Precipitation Index and North Atlantic Oscillation. *J. Hydrol.* **2015**, *526*, 136–150. [[CrossRef](#)]
44. Kim, T.; Valdes, J.B. Nonlinear model for drought forecasting based on a conjunction of wavelet transforms and neural networks. *J. Hydrol. Eng.* **2003**, *8*, 319–328. [[CrossRef](#)]
45. Mishra, A.; Desai, V.; Singh, V. Drought forecasting using a hybrid stochastic and neural network model. *J. Hydrol. Eng.* **2007**, *12*, 626–638. [[CrossRef](#)]
46. Ozger, M.; Mishra, A.; Singh, V. Long lead time drought forecasting using a wavelet and fuzzy logic combination model: A case study in Texas. *J. Hydrometeorol.* **2012**, *13*, 284–297. [[CrossRef](#)]
47. Bacanlı, U.; Firat, M.; Dikbas, F. Adaptive neuro-fuzzy inference system for drought forecasting. *Stoch. Environ. Res. Risk Assess.* **2009**, *23*, 1143–1154. [[CrossRef](#)]
48. Farokhnia, A.; Morid, S.; Byun, H.R. Application of global SST and SLP data for drought forecasting on Tehran plain using data mining and ANFIS techniques. *Theor. Appl. Climatol.* **2011**, *104*, 71–81. [[CrossRef](#)]
49. Mishra, A.K.; Singh, V.P. Drought modeling—A review. *J. Hydrol.* **2011**, *403*, 157–175. [[CrossRef](#)]
50. Agresti, A. *Categorical Data Analysis*; J. Wiley & Sons: New York, NY, USA, 1990.
51. Schneider, U.; Becker, A.; Meyer-Christoffer, A.; Ziese, M.; Rudolf, B. *Global Precipitation Analysis Products of the GPCC*; Global Precipitation Climatology Centre (GPCC): Boulder, CO, USA, 2010.
52. Trenberth, K.E.; Dai, A.; van der Schrier, G.; Jones, P.D.; Briffa, K.R.; Sheffield, J. Global warming and changes in drought. *Nat. Climate Chang.* **2014**, *4*, 17–22. [[CrossRef](#)]
53. Razei, T.; Martins, D.; Bordi, I.; Santos, J.F.; Portela, M.M.; Pereira, L.S.; Sutera, A. SPI modes of drought spatial and temporal variability in Portugal: Comparing observations, PT02 and GPCC gridded datasets. *Water Resour. Manag.* **2015**, *29*, 487–504. [[CrossRef](#)]
54. Paulo, A.A.; Pereira, L.S. Drought concepts and characterization: Comparing drought indices applied at local and regional Scales. *Water Int.* **2006**, *31*, 37–49. [[CrossRef](#)]
55. McKee, T.B.; Doesken, N.J.; Kleist, J. Drought monitoring with multiple time scales. In Proceedings of 9th Conference on Applied Climatology, Dallas, TX, USA, 15–20 January 1995; pp. 233–236.
56. Moreira, E.E.; Paulo, A.A.; Pereira, L.S.; Mexia, J.T. Analysis of SPI drought class transitions using log-linear models. *J. Hydrol.* **2006**, *331*, 349–359. [[CrossRef](#)]
57. Jolliffe, I.T.; Stephenson, D.B. *Forecast Verification: A Practitioner's Guide in Atmospheric Science*; Wiley: Hoboken, NJ, USA, 2003.
58. Nelder, J.A. Log-linear models for contingency tables: A generalization of classical least squares. *Appl. Stat.* **1974**, *23*, 323–329. [[CrossRef](#)]

